Supplementary Information

Article title

Smartphone-based fluorescent diagnostic system for highly pathogenic H5N1 viruses

Article author

Seon-Ju Yeo, Kyunghan Choi, Bui Thi Cuc, Nguyen Ngoc Hong, Duong Tuan Bao, Nguyen Minh Ngoc, Mai Quynh Le, Nguyen Le Khanh Hang, Nguyen Co Thach, Shyam Kumar Mallik, Hak Sung Kim, Chom-Kyu Chong, Hak Soo Choi, Haan Woo Sung, Kyoungsik Yu, Hyun Park

Supplementary Methods

Supplementary Figures

Supplementary Methods

Reflector Design

The light collection efficiency of the system using the reflective concentrator was much higher than that of the system without such a structure. Mainly because of the small aperture size of the smartphone's camera module, only a small portion of the fluorescent light (0.0091%) can be collected by the smartphone's camera when it is placed 53 mm above the lateral flow kit without the reflectors. Simple insertion of the reflector structure can significantly improve the fluorescent collection efficiency. Ray-tracing simulations (OpticStudio Professional Edition, Zemax, LLC, USA) were performed to determine the optimal CPC length, L, and its radius, a, for high light collection efficiency (Supplemental Fig. 1a). This simulation can trace the fluorescence light radiating from the fluorophore toward the detector, and calculate the fraction of the total collected power arrived at the detector. Since the lateral flow strip width is approximately 4 mm, the input aperture radius for the reflector is decided to be 2 mm. Considering the millimeter-level alignment tolerances for the field test situations while allowing the room for emission filter insertion, we use θ=15°, $a=p/\sin\theta$ =7.73 mm, and $L=(a+p)/\tan\theta$=36.3 mm for the upper CPC. The overall reflector structure size is relatively small, and its total height including the bottom parabolic mirror is 53 mm. The effective input aperture radius for the smartphone used in our experiment is smaller than 1 mm, and does not capture the whole output light from the reflective light concentrator as shown in Supplemental Fig. 1b. This is mainly because of the mismatch between the aperture sizes, a and p. The light detection efficiency can be significantly improved with the photodetectors with larger input apertures.

Bioconjugation of coumarin-derived dendrimer and antibody without latex bead

For conjugation with coumarin-derived dendrimer and anti-Influenza NP, 200 μL of 1 mg/mL antibody was mixed with 200 μL of conjugation buffer (0.1 M sodium bicarbonate, pH 8.5) at room temperature with shaking for 30 minutes. Coumarin-derived dendrimer (1 mg/mL) was dissolved in DMSO and 25 μL of coumarin-derived dendrimer (1mg/mL) (10 molar-fold excess of dye to antibody) was reacted with antibody at 4 °C for 4 hours. After finishing reaction, Zeba™ Spin Desalting columns (Thermo Fisher Scientific), 7K MWCO, were used for desalting by spinning down at 1,000 × g for 2 min. To block non-specific reaction, 1.5% of BSA was added to eluent. The final eluent was stored at 4 °C for testing.

Supplementary Figures

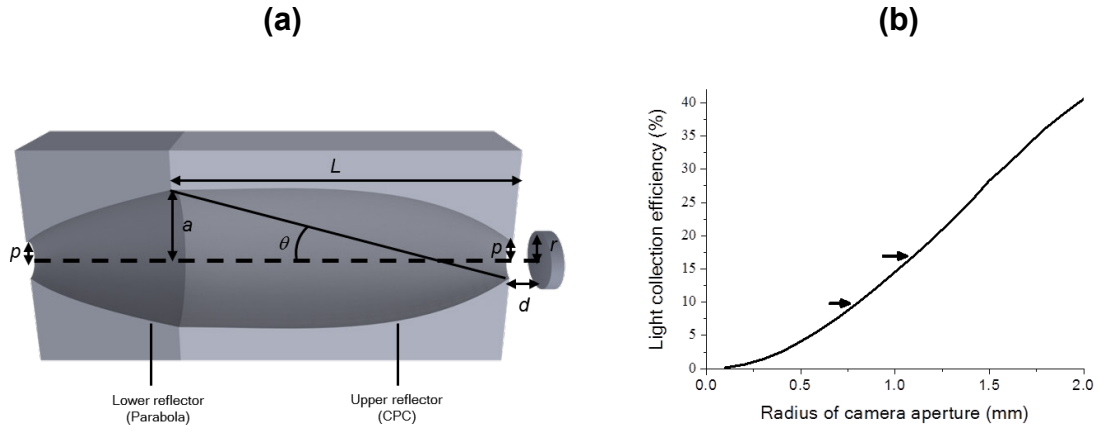

Figure S1. Efficiency of light collection. (a) Non-imaging reflector design parameters. (b) Light collection efficiency as a function of the photodetector aperture radius. The left arrow indicates the aperture radius used for our experiments. However, more recent smartphones tend to have larger aperture cameras for better image quality, and an example (Galaxy S6, Samsung Electronics, Suwon, Republic of Korea) is indicated by the right arrow, which shows a larger efficiency.

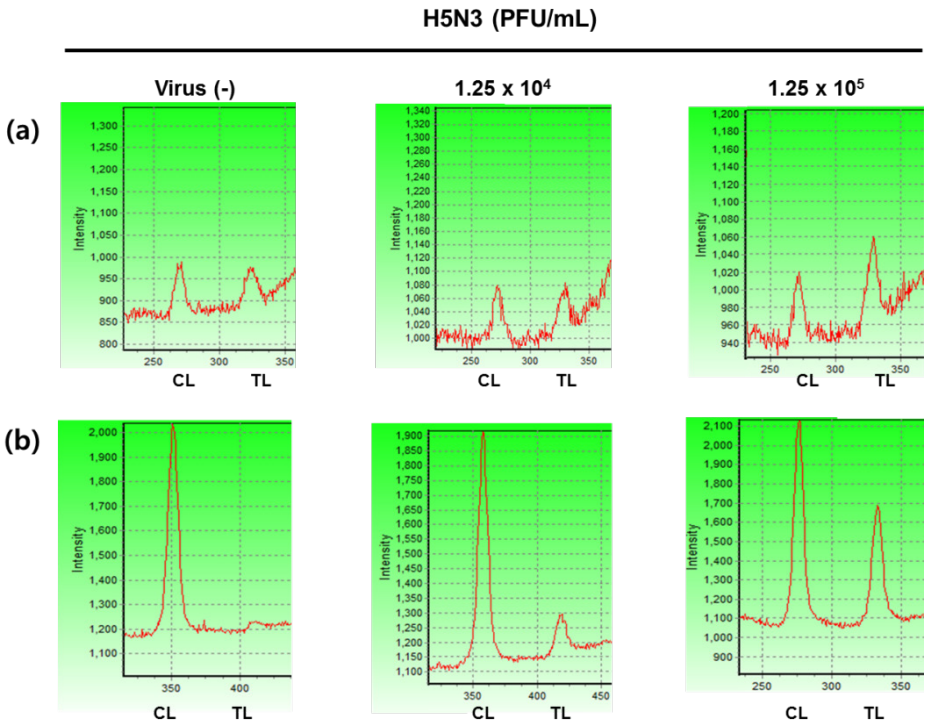

Figure S2. Efficiency of latex bead conjugation in FICT assay. Anti-influenza NP and coumarin-derived dendrimer was conjugated without latex bead (a) and with latex bead (b). By adaptation of latex bead to conjugation method, bioconjugate performance was enhanced, comparing to that of bioconjguate of coumarin-derived dendrimer and antibody without latex bead. Measurement of high virus titer (1.25×10^5 PFU/mL) was significantly different TL/CL values in both methods but the result of low virus titer (1.25×10^4 PFU/mL) was significantly different in only latex bead conjugation.

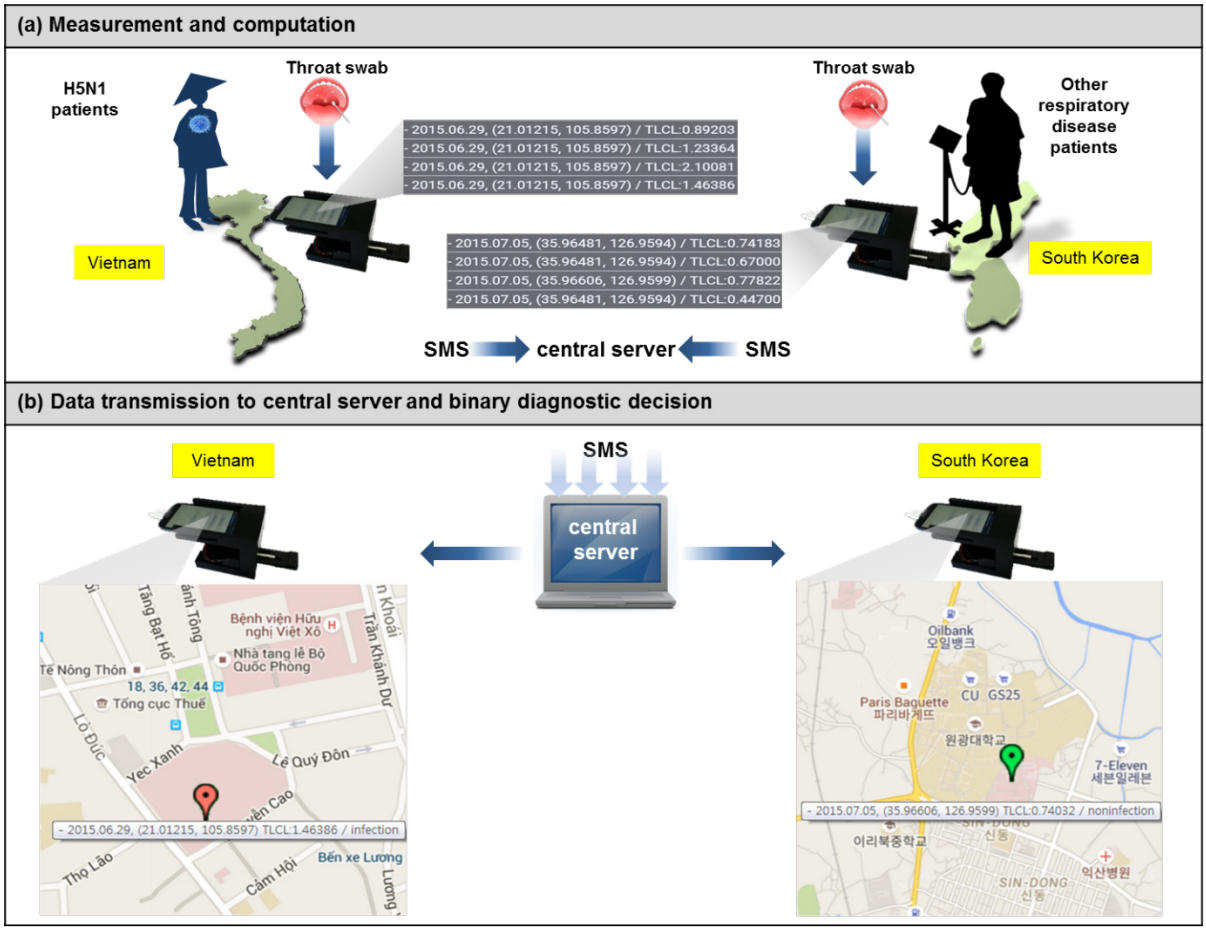

Fig. S3. Smartphone-based measurement and reporting of fluorescent immunoassay. (a) Users applied 75 μL of throat swab specimen of H5N1-confirmed patients and H5N1-negative patients to smartphone-based diagnostic devices in two different countries (Vietnam and Republic of Korea). After finishing the measurements, the test results were transmitted to the central computer server via wireless communication using SMS; the data were collected and stored in the database. (b) After analyzing the measurements according to the cut-off value (0.84), the test results were uploaded to the web server, generating a web-based H5N1 disease map; such a map can be used to monitor a worldwide H5N1 outbreak in real time. The color-coded labels indicate the measurement locations and detailed result information. The map can be zoomed-in to show detailed geographical information.

Table S1. Clinical raw data of TL/CL. Adenovirus (Adeno), parainfluenza virus (PIV), respiratory syncytial virus (RSV), and metapneumovirus (MPV)

Specimen #	Institute	RT-PCR	latitude	longitude	TL/CL
1	NIHE	H5N1	21.01	105.86	0.89
2	NIHE	H5N1	21.01	105.86	1.45
3	NIHE	H5N1	21.01	105.86	1.65
4	NIHE	H5N1	21.01	105.86	1.75
5	NIHE	H5N1	21.01	105.86	1.86
6	NIHE	H5N1	21.01	105.86	1.29
7	NIHE	H5N1	21.01	105.86	1.11
8	NIHE	H5N1	21.01	105.86	0.85
9	NIHE	H5N1	21.01	105.86	1.87
10	NIHE	H5N1	21.01	105.86	0.98
11	NIHE	H5N1	21.01	105.86	1.36
12	NIHE	H5N1	21.01	105.86	0.78
13	NIHE	H5N1	21.01	105.86	1.49
14	NIHE	H5N1	21.01	105.86	0.92
15	NIHE	H5N1	21.01	105.86	1.42
16	NIHE	H5N1	21.01	105.86	1.78
17	NIHE	H5N1	21.01	105.86	1.61
18	NIHE	H5N1	21.01	105.86	0.89
19	NIHE	H5N1	21.01	105.86	1.71
20	NIHE	H5N1	21.01	105.86	1.23
21	NIHE	H5N1	21.01	105.86	1.04
22	NIHE	H5N1	21.01	105.86	2.10
23	NIHE	H5N1	21.01	105.86	1.54
24	NIHE	H5N1	21.01	105.86	1.46
25	NIHE	H5N1	21.01	105.86	1.15
26	NIHE	H5N1	21.01	105.86	1.56
27	NIHE	H5N1	21.01	105.86	0.89
28	NIHE	H5N1	21.01	105.86	1.48
29	NIHE	H5N1	21.01	105.86	1.04
30	NIHE	Negative	21.01	105.86	0.59
31	NIHE	Negative	21.01	105.86	0.70
32	NIHE	Negative	21.01	105.86	0.55
33	NIHE	Negative	21.01	105.86	0.56
34	NIHE	Negative	21.01	105.86	0.38
35	NIHE	Negative	21.01	105.86	0.47
36	NIHE	Negative	21.01	105.86	0.78
37	NIHE	Negative	21.01	105.86	0.72
38	NIHE	Negative	21.01	105.86	0.83
39	NIHE	Negative	21.01	105.86	0.60
40	NIHE	Negative	21.01	105.86	0.62

41	NIHE	Negative	21.01	105.86	0.68
42	NIHE	Negative	21.01	105.86	0.64
43	NIHE	Negative	21.01	105.86	0.56
44	NIHE	Negative	21.01	105.86	0.44
45	NIHE	Negative	21.01	105.86	0.50
46	NIHE	Negative	21.01	105.86	0.53
47	NIHE	Negative	21.01	105.86	0.72
48	NIHE	Negative	21.01	105.86	0.56
49	NIHE	Negative	21.01	105.86	0.52
50	NIHE	Negative	21.01	105.86	0.63
51	NIHE	Negative	21.01	105.86	0.52
52	NIHE	Negative	21.01	105.86	0.48
53	NIHE	Negative	21.01	105.86	0.43
54	NIHE	Negative	21.01	105.86	0.61
55	NIHE	Negative	21.01	105.86	0.62
56	NIHE	Negative	21.01	105.86	0.72
57	NIHE	Negative	21.01	105.86	0.43
58	NIHE	Negative	21.01	105.86	0.71
59	Wonkwang	Adeno	35.97	126.96	0.71
60	Wonkwang	Adeno	35.97	126.96	0.68
61	Wonkwang	Adeno	35.97	126.96	0.6
62	Wonkwang	Adeno	35.97	126.96	0.41
63	Wonkwang	Adeno	35.97	126.96	0.76
64	Wonkwang	Adeno	35.97	126.96	0.65
65	Wonkwang	Adeno	35.97	126.96	0.66
66	Wonkwang	Adeno	35.97	126.96	0.69
67	Wonkwang	Adeno	35.97	126.96	0.74
68	Wonkwang	Adeno	35.97	126.96	0.7
69	Wonkwang	PIV	35.97	126.96	0.71
70	Wonkwang	PIV	35.97	126.96	0.66
71	Wonkwang	PIV	35.97	126.96	0.81
72	Wonkwang	PIV	35.97	126.96	0.75
73	Wonkwang	PIV	35.97	126.96	0.82
74	Wonkwang	PIV	35.97	126.96	0.75
75	Wonkwang	PIV	35.97	126.96	0.81
76	Wonkwang	PIV	35.97	126.96	0.78
77	Wonkwang	PIV	35.97	126.96	0.55
78	Wonkwang	PIV	35.97	126.96	0.94
79	Wonkwang	RSV	35.97	126.96	0.74
80	Wonkwang	RSV	35.97	126.96	0.73
81	Wonkwang	RSV	35.97	126.96	0.76
82	Wonkwang	RSV	35.97	126.96	0.52
83	Wonkwang	RSV	35.97	126.96	0.74
84	Wonkwang	RSV	35.97	126.96	0.68

85	Wonkwang	RSV	35.97	126.96	0.67
86	Wonkwang	RSV	35.97	126.96	0.72
87	Wonkwang	RSV	35.97	126.96	0.78
88	Wonkwang	RSV	35.97	126.96	0.81
89	Wonkwang	MPV	35.97	126.96	0.45
90	Wonkwang	MPV	35.97	126.96	0.64
91	Wonkwang	MPV	35.97	126.96	0.76
92	Wonkwang	MPV	35.97	126.96	0.82
93	Wonkwang	MPV	35.97	126.96	0.61
94	Wonkwang	MPV	35.97	126.96	0.54
95	Wonkwang	MPV	35.97	126.96	0.81
96	Wonkwang	MPV	35.97	126.96	0.77
97	Wonkwang	MPV	35.97	126.96	0.75
98	Wonkwang	MPV	35.97	126.96	0.62